A Generic Lie Group Model for Computer Vision

Within this research track we follow a generic Lie group approach to computer vision based on recent physiological research on how the primary visual cortex in the brain performs its unsurpassed pattern recognition capabilities, especially in noisy, low-contrast images with overlapping structures. This cortical modeling approach can be emulated by sophisticated mathematical models, involving stochastic processes, reproducing kernel theory, control theory, and (partial) differential equations on Lie-groups. Previous work has demonstrated the power of this general approach (developed by Remco Duits and co-workers within IST/e) in the specific context of orientation analysis of grey-scale images via ``invertible orientation scores" which provides a full overview of how an image is decomposed out of (multiple) local orientations.

We are currently extending this framework to higher dimensional orientation scores, scale and orientation scores, frequency scores (see Figure 1) and velocity scores and to recent novel complex image modalities (DW-MRI). We exploit these scores, their survey of multiple features per position, their group structures, and their intrinsic invertibility.

The main advantage of our approach compared to existing methods lies in the following combination

- We score the data coherently in a score which is a complex-valued function on an affine Lie group G beyond position space,
- We allow a stable reconstruction, so that we do not tamper data-evidence before processing takes place in G,
- We consider the context of features in G and amplify only the coherent features via contextual processing via *left-invariant* evolutions (diffusions and HJB-equations) on the score,
- We extract optimal curves in G via geometrical control theory based on the enhanced/evolved sores,
- We generically deal with the processing of multiple features (e.g. crossing lines, crossing textures, occlusions), without the involvement of ad-hoc classification of complex structures such as crossings.

We have already outperformed many methods in applied medical imaging and we aim for *a complete Lie group theoretical underpinning for perceptual organization in vision.*

For an illustration of the *practical benefits of left-invariant processing via scores* see Figure 1& 2 (cases G=SE(2),H(5),SIM(2)), see Figure 3 (case G=SE(2)) and see Figure 4, 5 and 6 (case G=SE(3), DW-MRI) ,

NB.
SE(d) = Lie group of rigid body motions,
SIM(2) = Lie group of translations and planar rotations and scalings,
H(5) = 5-dim. Heisenberg group.

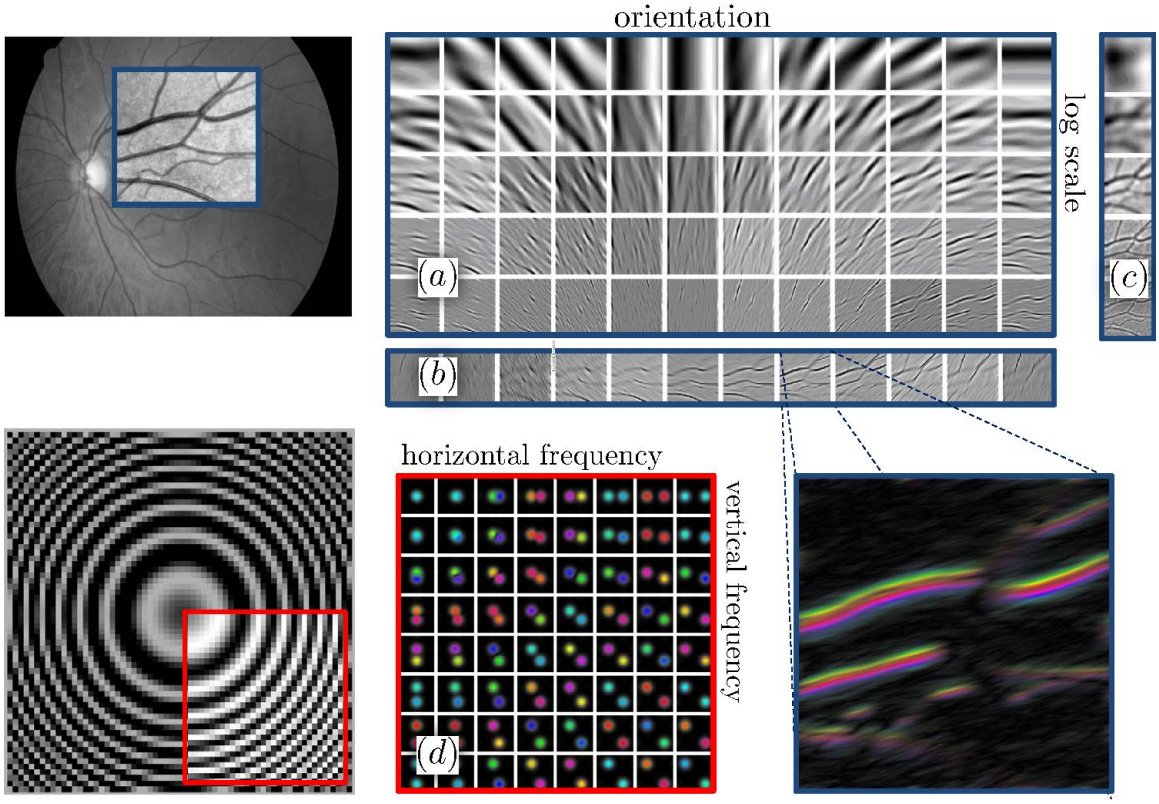

Figure 1 Left: original images with region of interest. Right : flat visualizations of scores defined on specific Lie groups . (a) real part of multiple scale orientation score (G=SIM(2)) , (b) real part of invertible orientation score (G=SE(2)) , (c) scale space representation, (d) frequency score (G=H(5)) with color coded phase. Bottom right: one slice in orientation score with color coded phase (distinguishing lines and edges).

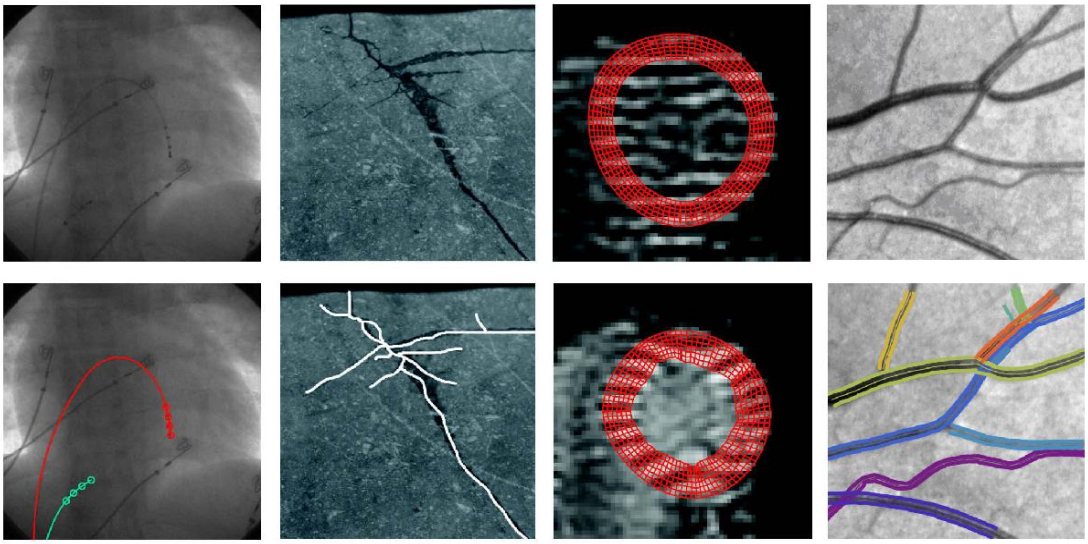

Figure 2 Various applications of (left-invariant) processing (detection) via scores. From left to right: 1.Detection of catheters in low-contrast X-ray fluoroscopy images via orientation scores, 2. Crack detection in granite stone slabs via orientation scores , 3. Quantification cardiac wall deformations via frequency scores, 4.Detection of the branching retinal vascular structure via (multiple scale) orientation scores outperforms the state of the art algorithms.

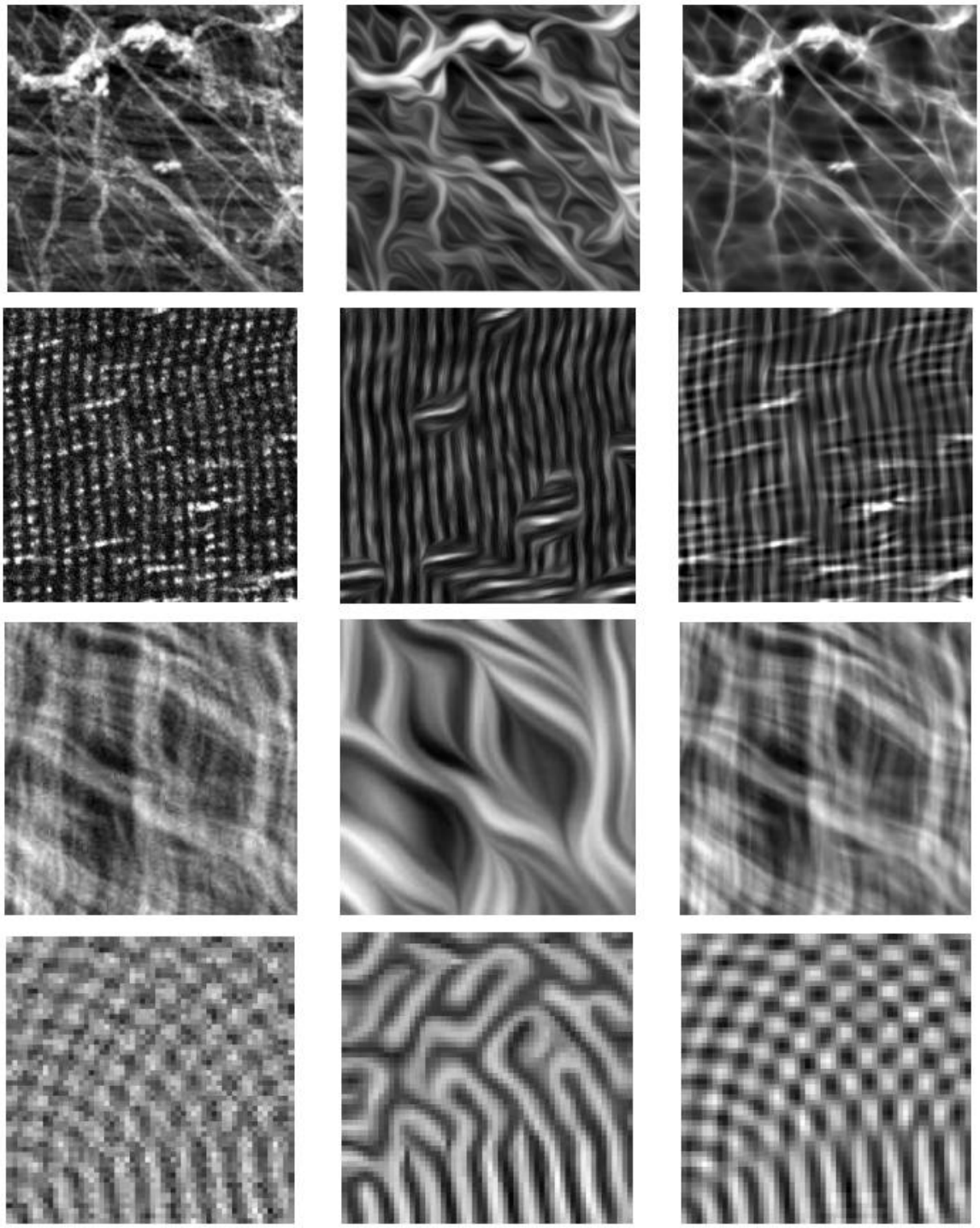

Figure 3 Left-invariant processing via invertible orientation scores is the right approach to deal with crossings and bifurcations in practice. Left column: original images. Middle column: result of standard coherence enhancing diffusion applied directly in the image domain (CED).
Right column: coherence enhancing diffusion via invertible orientation score (CED-OS),
1st row: 2-photon microscopy image of bone tissue. 2nd row: 2-photon microscopy image of muscle cell.
3rd row : collagen fibers of the heart. 4th row: artificial noisy interference pattern. Typically, these applications clearly show that coherence enhancing diffusion on orientation scores (CED-OS) is capable of handling crossings and bifurcations, whereas (CED) produces spurious artefacts at such junctions.

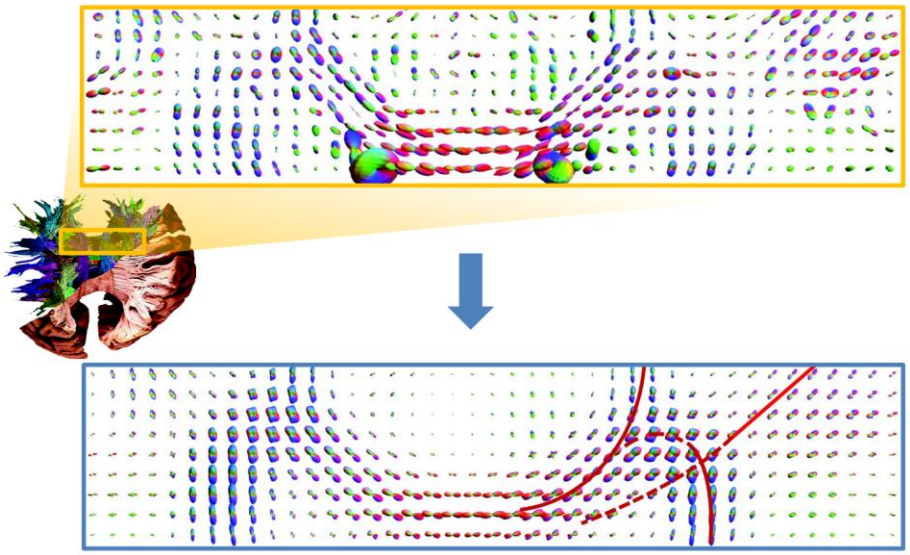

Figure 4 DW-MRI provides a field of angular diffusivity profiles of water molecules that follow biological fibers in brain white matter. Inevitable measurement errors induce some profiles that are poorly aligned with neighboring profiles. Scanning time limitations impose limited angular resolution so that complex-fiber structures (crossings) are poorly represented. Therefore contextual processing is needed. Here we applied contextual processing via a concatenation of a left-invariant HJB-system (erosion) and an adaptive diffusion on the coupled space of position and orientation (that is the Lie group quotient $SE(3)/(\{0\} \times SO(2))$) .

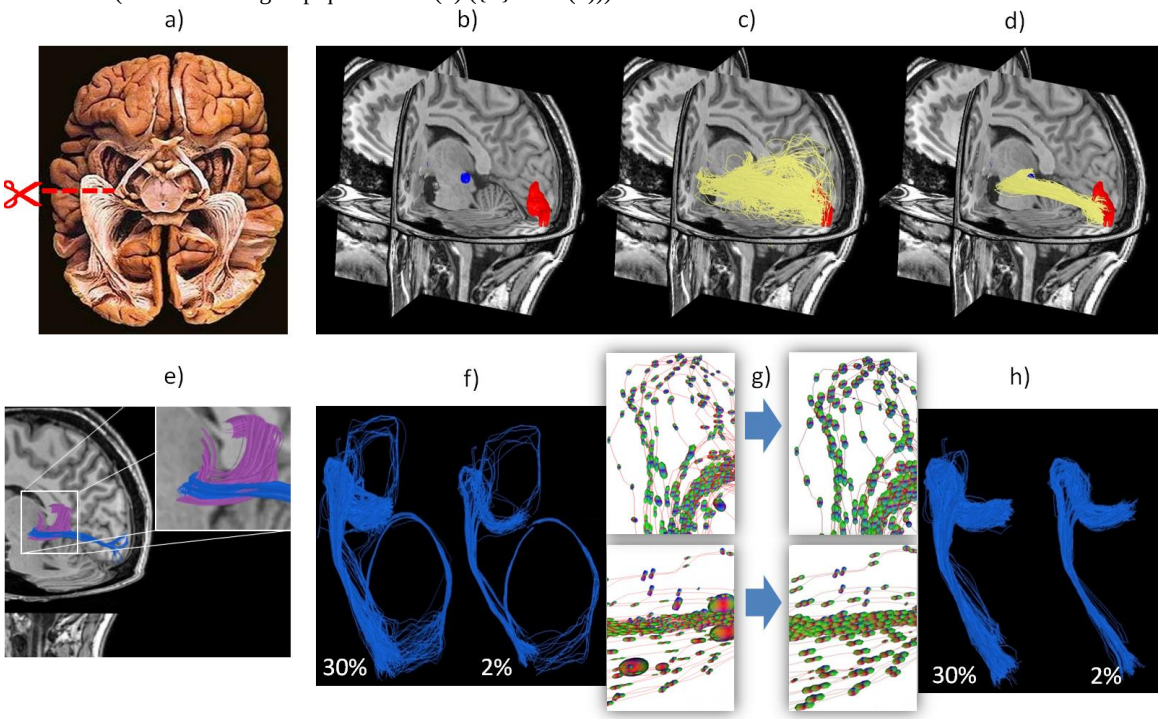

Figure 5 Illustration of how contextual processing via Lie group SE(3) depicted in Figure 1 makes a serious difference in a neuro image application (epilepsy surgery). a) In treating epilepsy surgeons should not damage the optic radiation fibers (OR) as they are responsible for the patient's visual sight. b) via fMRI we know where the OR starts (V1,calcarine sulcus in red) and ends (LGN in blue). c) probabilistic fiber tracking methods such as *contrack* generate an incredible amount of tracts selecting only those tracts that start in V1 and end in LGN. This produces a wild cluther of tracts. d) We score these tracts using the enhanced DW-MRI data and select the OR. This is difficult as there are many crossing/nearby fibers that complicate the tracking, see e). State of the art scoring of tracts based on original DW-MRI produces many errors (anatomically implausible tracts), whereas scoring of tracts based on our contextually processed DW-MRI selects the OR (exterior, posterior and anterior par, including Meyer's loop) perfectly.

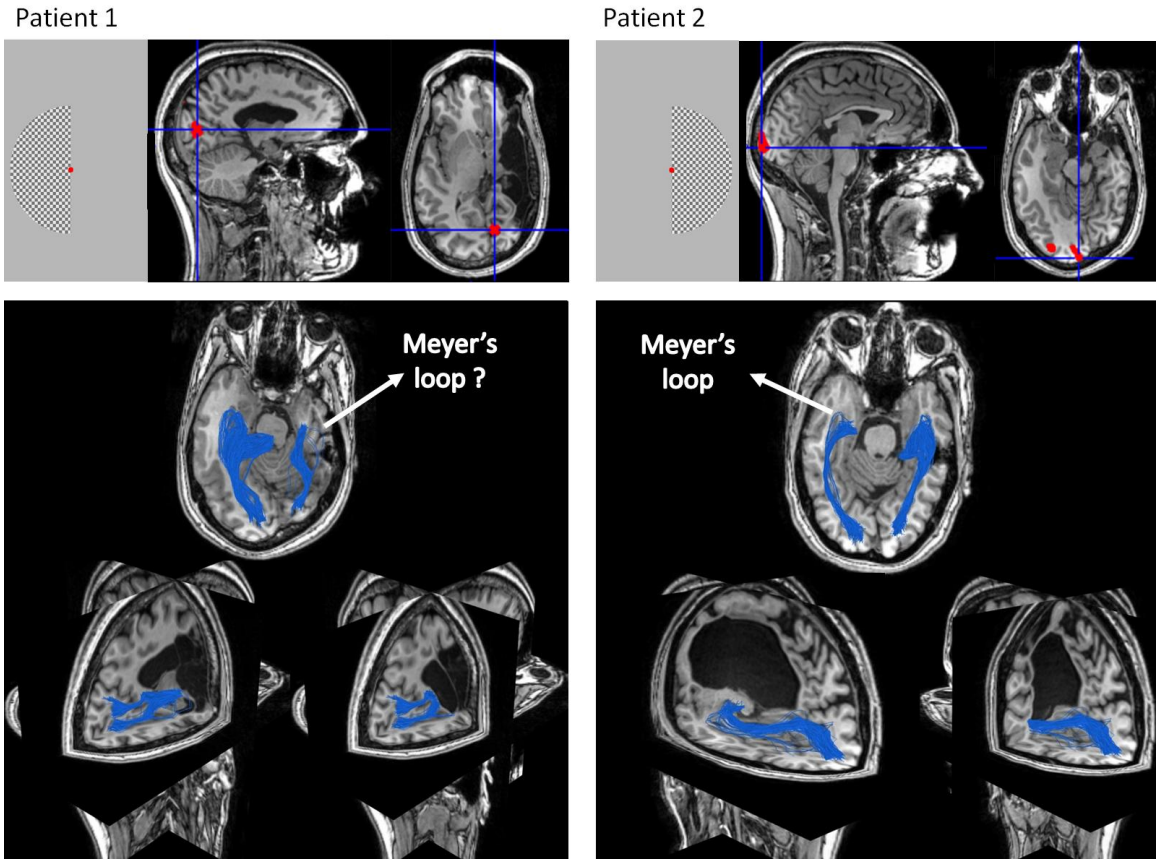

Figure 6 The same approach of scoring optic radiation fiber tracts as in Figure 3, only this time applied on difficult cases, where the neural anatomy of patients differs dramatically from the standard anatomy (due to large space occupying lesions). fMRI activation upon visual stimulation with checkerboard pattern. For both patients, visual activity became apparent in the pathological hemisphere, which allowed us to draw seed points in V1 for fiber tracking.